Structural and Functional Mapping of the Thrombin Domain Involved in the Binding to the Platelet Glycoprotein Ib[†]

Raimondo De Cristofaro,*[,§] Erica De Candia,[§] Raffaele Landolfi,[§] Sergio Rutella,[‡] and Scott W. Hall[#]

Hemostasis Research Center, Department of Internal Medicine, and Department of Hematology, Catholic University School of Medicine, Rome, Italy, and Division of Hematology, Stanford University, Stanford, California 94305, USA

Received March 9, 2001; Revised Manuscript Received July 5, 2001

ABSTRACT: The activation of human platelets by α-thrombin is mediated in part by cleavage of the protease-activated receptor (PAR) 1 and 4 and by the glycoprotein Ibα, (GpIbα), which binds with high affinity to α-thrombin. Recent studies have shown that the thrombin domain referred to as heparin binding site (HBS) is involved in the interaction with the platelet GpIbα. The HBS is rich in basic amino acids. To identify the key amino acid residues involved in the binding to GpIbα, we have performed alanine scanning mutagenesis of the basic HBS R93, R97, R101, R233, K236, K240, R233/K236/Q239, as well as of the neutral Q239 residues, located in different regions of the domain. For comparison, mutation at R67 within the fibrinogen recognition site (FRS) of thrombin was performed as well. Solid-phase binding experiments showed that the K_d of thrombin−GpIb interaction was reduced 22-fold for R93A, 8-fold for R97A, 13-fold for R101A, 29-fold for R233A, 21-fold for K236A, 5-fold for K240A, and 31-fold for the triple mutant R233A/K236A/Q239A, while the Q239A and R67A forms did not show any significant affinity change. The platelet activating capacity of these mutants was evaluated as well. Using gel-filtered platelets, the EC_{50} value of thrombin-induced aggregation was from 5- to 13-fold higher in the HBS mutants than in the WT form, and was linearly and positively correlated with the corresponding K_d values pertaining to thrombin binding to GpIb. Measurements of PAR-1 hydrolysis on the platelet membrane showed that the HBS mutants R233A, R101A, R93A, K236A, and R233/K236/Q239 forms had a reduction of the apparent k_{cat}/K_m value. These results are a consequence of a defective binding to GpIb, which is known to optimize the interaction with PAR-1 in situ. A confirm of this hypothesis came from the demonstration that the k_{cat}/K_m value pertaining to the hydrolysis by the HBS-mutated thrombins of the synthetic PAR-1 38−60 peptide in solution was similar to that one obtained with the WT form. In conclusion, these experiments provide a structural and functional mapping of the thrombin HBS subregions involved in the binding to the platelet GpIbα and in the cell activation.

INTRODUCTION

Platelet glycoprotein Ib (GpIb)[1] belongs to the so-called "leucine-rich repeat" family of proteins and binds to von Willebrand factor, thus allowing the early adhesion of platelets to exposed subendothelium at high shear rates (*1*−*3*). In addition, GpIb also binds to thrombin with high affinity (*4*). The inhibition of this interaction reduces thrombin-induced platelet activation through a reduction in PAR-1 cleavage rate (*5*) and probably through other still unknown mechanisms. GpIb is a 150-kDa transmembrane glycoprotein and contains a 27-kDa β-subunit connected via a disulfide bond to the α-subunit (*6*−*7*). Glycocalicin (GC), the 140-kDa extracytoplasmic portion of GpIbα, that bears the von Willebrand factor and thrombin binding sites, is generated by the hydrolysis of GpIbα with endogenous calcium-dependent sulfydryl proteases, such as calpain (*8*). Recent studies have shown that the GpIbα thrombin binding site maps to an acidic C-terminal region spanning residues D272 to E282 (*4*, *9*). Moreover, recent studies indicate that thrombin binds to GpIb via its heparin binding site (HBS) (*5*, *9*−*11*). This conclusion was achieved with functional experiments that showed that GpIb binding to thrombin inhibits the heparin-catalyzed enzyme inhibition by anti-thrombin III (*9*). Moreover, several ligands for HBS inhibit the enzyme interaction with GpIb, and, in addition, some thrombin forms mutated at HBS, namely, the R101A, the R93A and the K236A thrombin mutants, have a reduced interaction with GpIb (*5*, *11*).

To provide a structural mapping of the thrombin residues involved in binding to GpIbα, we performed an alanine scanning mutagenesis of cationic and neutral residues contained in the thrombin HBS. The recombinant thrombin forms were mutated at R93, R97, R101, R233, K236, Q239,

* Address correspondence to this author at Centro Ricerche Fisiopatologia dell'Emostasi, Istituto di Semeiotica Medica, Università Cattolica S. Cuore Largo F. Vito 1, 00168 Roma, Italy. Phone: (+39)-06-30154438. FAX: (+39)-06-35503777. E-mail: rdecristofaro@rm.unicatt.it.

[†] This study was financially supported by a grant "COFIN 2000" of the Ministry of the University and Scientific and Technological Research of Italy (R.D.C.).

[§] Hemostasis Research Center, Catholic University School of Medicine.

[‡] Department of Hematology, Catholic University School of Medicine.

[#] Stanford University.

[1] Abbreviations: GC, glycocalicin; GpIb, glycoprotein Ib; HBS, heparin binding site; PAR, protease activated receptor; PAR1P, PAR-1 38−60 peptide.

10.1021/bi010491f CCC: $20.00
Published on Web 10/13/2001

R233/K236/Q239, and K240 (chymotrypsin numbering system). In addition, mutation within the fibrinogen recognition site (FRS) of thrombin was performed at R67. Mutation of this residue has been observed in vivo, the so-called thrombin Quick I. This thrombin mutation impairs thrombin's interaction with several substrates including fibrinogen, thrombomodulin, and platelets (*12*−*13*). The properties of binding to GC of all the above mutants and their enzymatic properties pertaining to the hydrolysis of both the synthetic PAR-1 38−60 peptide (PAR1P) in solution and PAR-1 in situ were investigated as well. In addition, the activation of gel-filtered platelets by the thrombin mutants was determined by measuring their aggregation response. These experiments provide a structural and functional mapping of the thrombin HBS subregions involved in GpIbα binding, which contributes to a full platelet activation. The known crystal structure of the thrombin molecule allowed derivation of a 3D model of the thrombin surface region implicated in the GpIbα binding and platelet activation.

MATERIALS AND METHODS

Materials. The acethylated and amidated PAR-1_{38-60} peptide, LDPRSFLLRNPNDKYEPFWEDEE (PAR1P), was synthesized and characterized by mass spectrometry at Primm srl (Milan, Italy). Purified porcine erythrocytes calpain I was purchased from Calbiochem (San Diego, CA).

Thrombin Mutants. Mutant thrombins R93A, R97A, R101A, R233A, K236A, Q239A, K240A, R233A/K236A/Q239A, and R67A (chymotrypsin numbering system) and the wild type (WT) form were obtained and characterized as previously described (*13*). The full-length human prothrombin gene was inserted into the expression vector pRc/CMV (Invitrogen) and expressed in CHO AA8 cells, which were grown and passaged in CHO S-serum-free medium (Life Technologies, Inc.) containing 10% fetal bovine serum and 100 U/mL penicillin and 100 μg/mL streptomycin. WT and mutant prothrombins were activated to active thrombin using 50 μg/mL ecarin (Sigma-Aldrich) for 1 h at 37 °C. Purification of thrombins was accomplished by ion exchange FPLC, according to a previously detailed procedure (*13*). The HBS mutant forms retained their catalytic activity (see below), although their ability to interact with heparin was severely impaired, as demonstrated by in vitro studies on heparin-catalyzed thrombin inhibition by antithrombin III (all but the Q239A mutant), according to methods previously detailed (*9*). SDS−PAGE on 8% gel showed that all the purified recombinant thrombins were pure and showed a molecular mass of about 35 kDa.

Steady-State Kinetics of Amidase Activity of WT and Mutant Thrombins toward a Synthetic Peptide Substrate. Steady-state kinetics of the hydrolytic reaction of the D-Phe−Pip−Pro−Arg-pNA substrate by WT and mutant thrombins was studied under the experimental conditions of 10 mM Tris-HCl, 0.15 M NaCl, 0.1% PEG 6000, pH 8.00, at 25 °C, according to a previously detailed procedure (*14*).

Purification of Platelet Glycocalicin and Solid-Phase Binding Studies. Platelet GC was prepared by using purified porcine erythrocytes calpaine I at 10 μg/mL to cleave the protein from washed platelets suspended in 10 mM Hepes, 0.135 M NaCl, 3 mM KCl, 100 μM $CaCl_2$. The hydrolytic reaction was stopped by addition of 0.5 mM EDTA. The calpain-treated platelets were precipitated by centrifugation at 1000*g* for 20 min. The supernatant was used to purify GC, which was obtained using a Mono Q FPLC column, as previously reported (*9*). Solid-phase binding studies were performed using glycocalicin immobilized on high-binding capacity polystyrene Immulon plates, as previously detailed (*10*), in 10 mM HEPES, 0.1 M NaCl, 0.1% PEG 6000, pH 7.5, at 25 °C. The GpIb-bound thrombin was detected by adding for 1 h 100 μM of the synthetic substrate D-Phe−Pip−Arg-pNA and reading the absorbance of the released *p*-nitroaniline at 405 nm. The equilibrium dissociation constant of the thrombin−GC interaction, K_d, was obtained by using the relation:

$$\mathrm{Abs_{obs}} = \mathrm{Abs_{max}}T/(K_d + T) \quad (1)$$

where $\mathrm{Abs_{obs}}$ is the observed absorbance value at 405 nm, $\mathrm{Abs_{max}}$ is the asymptotic absorbance value, and T is the thrombin concentration.

Measurement of the PAR1P Peptide Hydrolysis by WT and Mutant Thrombins. Hydrolysis of the PAR1P peptide (NH_2-LDPRSFLLRNPNDKYEPFWEDEE-COOH) by the different thrombin forms was followed by measuring the release of the peptide LDPR, resulting from the cleavage of the NH_2-terminus of PAR-1, according to a previously described method (*15*). Briefly, 0.5 μM PAR1P peptide was incubated with 50−100 pM WT or mutant thrombins (1 nM for the R67A form) in 10 mM HEPES, 0.15 M NaCl, 0.1% PEG 6000, pH 7.5, at 25 °C. At time intervals (1, 2, 3, 4, 8, 12, and 15 min), the reaction was stopped with 0.3 M $HClO_4$ and the cleaved peptide was measured by reversed-phase HPLC, using a 250 × 4.6 mm RP-304 column (Bio-Rad Laboratories, Hercules, CA), as previously detailed (*15*). The concentration of PAR1P peptide cleaved at time = t, P_t, were fitted to the following equation:

$$P_t = P_\infty[1 - \exp(-k_{obs}t)] \quad (2)$$

where P_∞ is the peptide concentration at $t = \infty$ and k_{obs} is the pseudo-first-order rate of PAR-1 hydrolysis, equal to e_0k_{cat}/K_m (e_0 is the thrombin concentration).

Preparation of Platelets and Aggregometry Studies. Platelets from normal donors were obtained by gel filtration of platelet-rich plasma onto Sepharose 2B columns (25 × 1 cm) equilibrated with a buffer containing 20 mM Hepes, 135 mM NaCl, 5 mM KCl, 5 mM glucose, 0.2% BSA, pH 7.4. The platelet count was adjusted to $2 \times 10^5/\mu$L with washing buffer in all the experiments. Gel filtered platelets were suspended in HEPES buffer, as detailed above, containing 1 mM $CaCl_2$ and used at a final count of 200 000/μL. Platelet aggregation by thrombin was studied using a four-channel PACKS-4 aggregometer (Helena Laboratories, Sunderland, UK), according to the turbidometric Born method. In some experiments, platelets were stimulated by recombinant human WT and mutant thrombins at concentrations ranging from 0.39 to 200 nM. The observed velocity of absorbance change, $\mathrm{Vel_{obs}}$, was measured and expressed as %/min. The EC_{50} values of thrombin, T, were calculated by fitting the data to the equation:

$$\mathrm{Vel_{obs}} = \frac{\mathrm{Vel_{max}}T}{(EC_{50} + T)} \quad (3)$$

Table 1: Best-fit K_m and k_{cat} Values Pertaining to the Hydrolysis of the D-Phe−Pip−Arg-pNA Substrate by the WT and Mutant Thrombin Forms

thrombin form	K_m (μM)	k_{cat} (s^{-1})	k_{cat}/K_m ($\times 10^7 M^{-1} s^{-1}$)
WT	1.9 ± 0.2	75 ± 2	3.95
R93	2.0 ± 0.3	73 ± 4	3.65
R97	2.3 ± 0.3	76 ± 3	3.30
R101	1.8 ± 0.2	70 ± 2	3.89
R233	1.5 ± 0.2	55 ± 2	3.67
K236	1.7 ± 0.2	60 ± 3	3.52
Q239	1.9 ± 0.1	65 ± 2	3.42
R233/K236/Q239	2.0 ± 0.1	59 ± 1	2.95
K240	1.8 ± 0.1	50 ± 1	2.78
R67	2.0 ± 0.2	65 ± 2	3.25

The best fit parameter values were obtained using the GRAFIT software (Erithacus software Ltd., Staines, U.K.) based on a modified Marquardt algorithm.

Measurement of PAR-1 Hydrolysis by WT and Mutant Thrombins on Intact Platelets. Gel filtered platelets were exposed to 1 nM of WT, R233A, R93A, R101A, R233/K236/Q239A and 10 nM R67A thrombin forms. The HBS mutated thrombin forms were used as thrombin forms lacking a normal interaction with GpIb (see below) to investigate how this defect could affect the PAR-1 hydrolysis in situ. On the other hand, the R67A form was used in these experiments since it was expected to have a defective interaction per se with PAR-1. At different times (from 15 to 600 s), aliquots of 50 μL of stimulated platelets were drawn into tubes containing 4 μM PPACK, which abolished the thrombin activity, and the tubes were placed in ice to stop internalization of cleaved PAR-1 molecules (*5*, *16*).

The presence of intact PAR-1 molecules on the platelet membrane at different times after thrombin stimulation was measured by using a phycoerythrin (PE)-conjugated anti-PAR-1 MoAb, SPAN12 clone (Immunotech), as previously detailed (*5*). The samples were run through a FACScan flow cytometer (Becton Dickinson, Mountain View, CA) equipped with an argon laser emitting at 488 nm. PE signals were collected and recorded at 575 nm. Levels of PAR-1 expression were measured in terms of geometric mean of specific fluorescence.

RESULTS

Steady-State Kinetics of Amidase Activity of WT and Mutant Thrombins toward a Synthetic Peptide Substrate. The recombinant WT and mutant thrombin forms showed similar Michaelis constants pertaining to the hydrolysis of the Phe−Pip−Arg-pNA substrate, as listed in Table 1. These experiments showed that the mutations did not alter the catalytic machinery of the enzyme. Any other modification of the amidase activity of the mutated thrombins was thus attributed to alterations concerning the various enzyme exosites, involved in macromolecular ligand interactions.

Binding of WT and Mutant Thrombins to Immobilized GC. Analysis of experimental data showed that WT thrombin binds to immobilized GC with a K_d value of 102 ± 8 nM at 100 mM NaCl, as shown in Figure 1 and in Table 2. This value was in good agreement with the K_d values previously determined for thrombin−GC and thrombin−GpIbα(1−282) interactions, both in solid-phase binding and functional experiments (*5*, *9*, *15*). The thrombin forms mutated at the HBS residues showed a severe reduction of GC affinity,

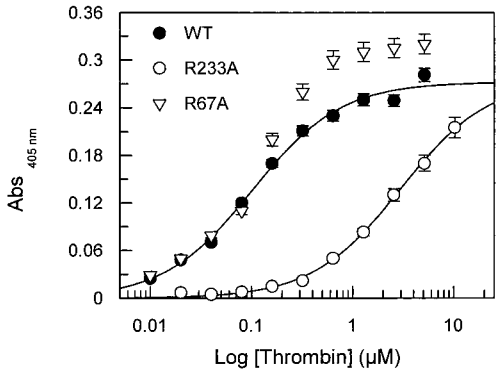

FIGURE 1: Solid-phase binding of WT, R233A, and R67A thrombin forms to immobilized GC. Continuous lines were drawn by fitting the experimental data to eq 1 with the best-fit K_d values listed in Table 1 and $Abs_{max} = 0.272 \pm 0.005$ for the WT (●) and $Abs_{max} = 0.275 \pm 0.007$ for the R233 form (○). The experimental points pertaining to the R67A mutant (▽) are shown for comparison. The experimental points are the mean from two different measurements, with the vertical bars representing the standard deviations.

Table 2: Best-fit K_d Values of GC Binding to WT and Mutant Thrombin Forms, with the Associated $\Delta\Delta G$ Values of Binding

thrombin form	K_d (μM)	$\Delta\Delta G$ (kcal/mol)[a]
WT	0.102 ± 0.01	0
R93	2.2 ± 0.3	1.8
R97	0.81 ± 0.1	1.2
R101	1.3 ± 0.05	1.5
R233	2.98 ± 0.18	2.0
K236	2.11 ± 0.2	1.79
Q239	0.11 ± 0.1	0.04
R233/K236/Q239	3.1 ± 0.4	2.01
K240	0.5 ± 0.06	0.94
R67	0.12 ± 0.02	0.1

[a] $\Delta\Delta G = RT \ln(K_d^M/K_d^\circ)$, where K_d^M and K_d° are the equilibrium dissociation constant pertaining to the mutant and the WT form, respectively, at 0.1 M NaCl, pH 7.50, and $T = 298$ K. R is the gas constant (1.9817 cal K^{-1} mol^{-1}).

except the Q239A mutant, which had a similar K_d value. The best-fit K_d values for all the thrombin forms are listed in Table 2. A representative binding curve pertaining to the R233A mutant is shown in Figure 1, which shows a right-shifted titration curve, consistent with a reduced affinity of the mutant for GpIb. In contrast, the R67A mutant did not show any significant affinity change as compared with WT thrombin.

Measurement of the PAR1P Peptide Hydrolysis in Solution by the WT and Mutant Thrombins. The experimental method previously detailed (*15*) allowed measurement of the k_{cat}/K_m value pertaining to the PAR1P hydrolysis by all the recombinant thrombin forms. A typical experiment is shown in Figure 2. The best-fit k_{cat}/K_m values along with the standard errors are listed in Table 3. A severe reduction of the k_{cat}/K_m value (29-fold) was observed with the R67A mutant, while the values of the HBS mutants were close to that measured for the WT form. These results are in agreement with the known involvement of the FRS in the PAR-1 ligation, whereas HBS residues are not involved in the interaction with the thrombin receptor, as previously suggested (*15*). It is noteworthy that the Q239A form, as compared to the WT species, showed an even higher k_{cat}/K_m value.

PAR-1 Hydrolysis by WT and Mutant Thrombins on Intact Platelets. Measurement of PAR-1 hydrolysis in situ was

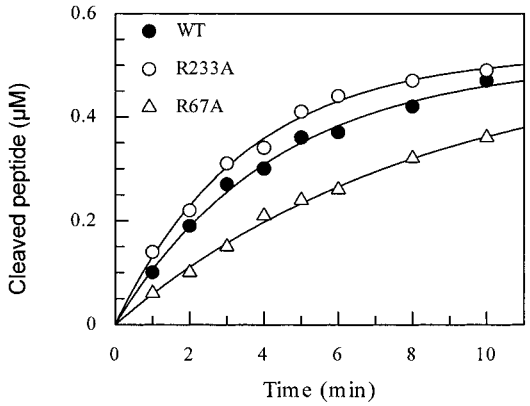

FIGURE 2: Kinetics of PAR-1 38−60 peptide hydrolysis in solution by the WT, R233A, and R67A forms. The peptide was used at 0.5 μM, the enzyme was at 50 pM for the WT and the R233A forms, whereas at 0.75 nM for the R67A mutant. The continuous lines were drawn according to eq 2, using the best-fit parameter values as listed in Table 3.

Table 3: Best-fit k_{cat}/K_m Values of PAR1P Hydrolysis in Solution, $(k_{cat}/K_m)^{sol}$, and PAR-1 Hydrolysis in Situ, $(k_{cat}/K_m)^{situ}$

thrombin form	$(k_{cat}/K_m)^{sol}$ ($\times 10^7\,M^{-1}\,s^{-1}$)	$(k_{cat}/K_m)^{situ}$ ($\times 10^7\,M^{-1}\,s^{-1}$)
WT	7.75 ± 0.7	1.15 ± 0.2
R93A	8.2 ± 1.0	0.2 ± 0.07
R97A	8.1 ± 0.9	ND[a]
R101A	9.6 ± 0.9	0.4 ± 0.05
R233A	9.7 ± 0.7	0.2 ± 0.04
K236A	11 ± 1.4	0.4 ± 0.05
Q239A	14 ± 1.2	ND
R233/K236/Q239A	11 ± 1.1	0.15 ± 0.03
K240A	11.5 ± 0.9	ND
R67A	0.27 ± 0.03	0.06 ± 0.01

[a] ND: not determined.

accomplished by a cytofluorimetric method, using a fluorescent monoclonal antibody, referred to as SPAN-12, as previously detailed (*5*). This MoAb recognizes only the intact N-terminal portion of the receptor, namely, the region cleaved by thrombin (*16*). After cleavage, the MoAb longer interacts with the receptor, so that disappearance of the MoAb signal reflects the hydrolytic reaction. Under the conditions used in the cytofluorimetric experiments, no platelet aggregation was observed, and no aggregates were seen in the FACS analysis. The kinetics of PAR-1 cleavage could be fitted to a single-exponential decay equation, whose rate constant, k_{obs}, is proportional to the k_{cat}/K_m value of thrombin PAR-1 hydrolysis, according to the relation $k_{obs} = e_0 k_{cat}/K_m$, where e_0 is the thrombin concentration (*5*).

The HBS mutants with most defective binding to GpIb, namely, R101A, R93A, R233A, K236A, and R233/K236/Q239A, were used in these experiments. All these mutants exhibited a 5−9-fold reduction of the k_{cat}/K_m value pertaining to PAR-1 hyrolysis in situ, as listed in Table 3.

In Figure 3, the kinetics of PAR-1 hydrolysis by the WT, the R233A, and the R67A mutants are reported. A severe defect was observed for the R67A mutant as well, whose k_{cat}/K_m value was 19-fold lower than in the WT species, as expected on the basis of impaired binding of this mutant thrombin to PAR-1. Moreover, taking into consideration the different experimental systems, the extent of this reduction was comparable to that one observed using PAR1P in solution.

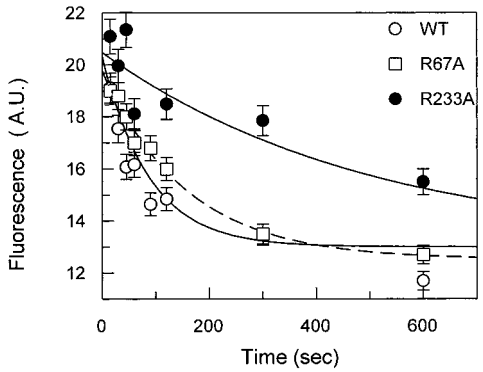

FIGURE 3: Kinetics of PAR-1 cleavage in situ by different thrombin forms. The experimental conditions are reported under Materials and Methods, using 40 000 gel-filtered platelets/μL and 0.12 μg/mL of the SPAN 12 MoAb. PAR-1 cleavage was measured as a loss of SPAN12 MoAb fluorescence over time (A. U. = arbitrary units). Both the WT and the R233A thrombin forms were used at 1 nM, while the R67A mutant was used at 10 nM. Continuous lines are drawn according to eq 2 with the best-fit k_{cat}/K_m values as reported in Table 3. Data are presented as mean ± SE from two different determinations.

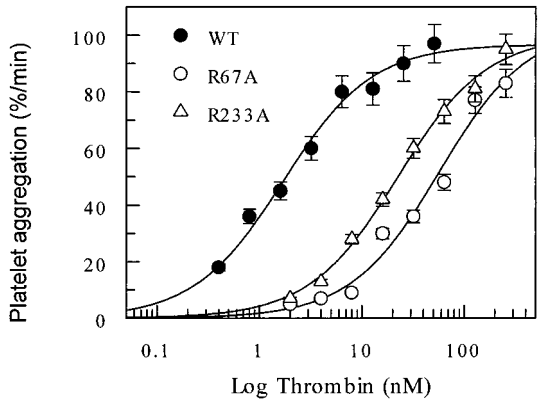

FIGURE 4: Effect of alanine mutation of thrombin R233 and R67 on the aggregation of gel-filtered platelets. Aggregation of gel-filtered platelets (200 000/μL) induced by WT thrombin as compared to that of both R233A and R67A mutants. Continuous lines were drawn using the best-fit EC_{50} values calculated by eq 3 and reported in Table 4.

Table 4: Best-fit EC_{50} Values of the WT and Mutant Thrombin-Induced Platelet Aggregation

thrombin form	EC_{50} (nM)
WT	1.7 ± 0.2
R93A	20.4 ± 3
R97A	8.5 ± 0.9
R101A	17 ± 2
R233	22.5 ± 1.9
K236	17.2 ± 3
Q239	1.0 ± 0.1
R233/K236/Q239	22 ± 3
K240	11.9 ± 1.5
R67	57.1 ± 12.2

Aggregometry Studies. The aggregometric studies were carried out to investigate the effects of the different thrombin mutations on the enzyme-induced platelet aggregation. Most of the thrombins mutated at the HBS showed a defective activating capacity, as shown in Figure 4 and Table 4, where the best-fit EC_{50} values are listed along with the standard errors. The only exception was the Q239A mutant, which had a lower EC_{50} value as compared to the WT form. Interestingly, the EC_{50} values were found to be positively

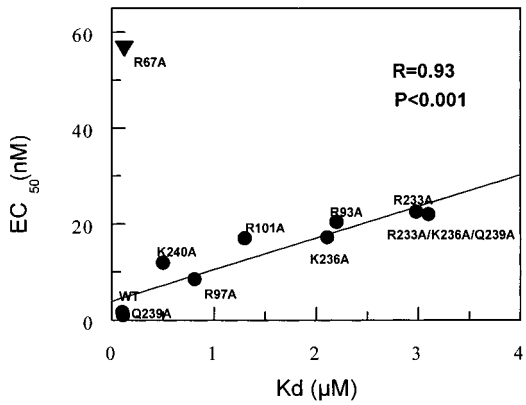

FIGURE 5: Correlation between the EC_{50} values of the thrombin-induced platelet aggregation by the recombinant forms indicated in the figure and the corresponding K_d values of the GpIb interaction. The straight line is a linear regression with the *R* and *P* values indicated in the figure. The experimental point pertaining to the R67A mutant is also shown for comparison.

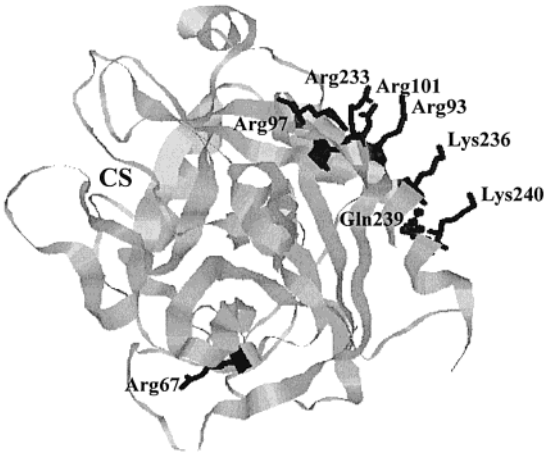

FIGURE 6: Ribbon plot of the crystal structure of human α-thrombin, solved at 1.9 Å by Bode et al. (*17*). The residues critical for GpIb binding are differently portrayed: HBS residues (Lys236, Lys240, Arg93, Arg97, Arg101, R233) as sticks in bold, except Q239, that is represented as balls and sticks. R67 at the FRS is shown as sticks in bold. CS indicates the pocket of the catalytic site.

correlated to the K_d values of thrombin−GpIb interaction, as shown in Figure 4. This finding confirms previous results, which showed that thrombin binding to GpIb is a necessary step for a full platelet activation (*5*). It is noteworthy that the experimental point pertaining to the R67A mutant does not follow the correlation line between the EC_{50} and K_d values, observed for the HBS mutants (Figure 5), due to the different functional defect of this thrombin form.

DISCUSSION

In this study, a collection of thrombin mutants was used to provide a structural mapping of the key residues involved in the enzyme interaction with platelet GpIb. Recent studies have shown that GpIb interacts with the HBS of thrombin (*5*, *9*−*11*). A very recent study by Li et al. has also shown that thrombin R93 and K236 residues are both involved in GpIb ligation (*11*). Thus, to identify other key residues engaged in the GpIb ligation and to provide a more extensive mapping of the enzyme interaction site, we produced by alanine scanning mutagenesis eight thrombin mutants bearing modifications of amino acid residues present in the HBS, namely, R93, R97, R101, R233, K236, Q239, K240, and R233/K236/Q239. In addition, as thrombin interacts with PAR-1 through its FRS, a mutant enzyme modified at R67, present in the FRS, was also produced and used as reference in enzymatic studies pertaining to PAR-1 cleavage. R67 is known to be important in mediating thrombin's interaction with fibrinogen, thrombomodulin, and platelet activation (*12*, *13*).

As shown in Table 1, all the above mutations did not inhibit the catalytic activity of the enzyme, since the Michaelis parameters pertaining to the steady-state hydrolysis of the Phe−Pip−Arg-pNA substrate did not undergo major changes. On the contrary, a severe affinity decrease for GpIb binding was observed for most of the HBS mutants. The only exception was the Q239A mutant, whose affinity was very close to that of the WT form. The largest affinity decrease was observed for the R233A, the triple R233A/K236A/Q239A, the R93A, and the K236 mutants (ranging from 22- to 31-fold). Significant affinity changes, although of minor extent, were also observed for the R97A and R240A, whereas intermediate affinity decrease were observed for the R101A form. The substitutions resulted in $\Delta\Delta G$ values of binding amounting from 0.04 (Q239A) to 2 kcal/mol (R233A and the triple R233/K236/Q239 mutant). The highest differences of the ΔΔG values of binding pertaining to the single-site mutants were observed for the R233A, R93A, K236A, and R101A forms. This may suggest that the basic cluster constituted by the R233/R93/R101 residues plays a key role in the energetics of GpIb interaction (Figure 6). These results allowed construction of a molecular map of the thrombin domain involved in GpIb binding. The enzyme interaction domain covers an extensive electropositive surface area (roughly equal to 200 $Å^2$), whose residues are well exposed to the solvent, as shown in Figure 6. The HBS of thrombin is the most electropositive region of the molecule (*17*), and this may be in agreement with the previously demonstrated large salt-dependency of the GpIb binding (*5*, *11*). The large electrostatic component of this binding may serve to correctly orient the interacting macromolecules, and might suggest, in the absence of detailed kinetic evidence, that thrombin−GpIb interaction could occur via a multistep mechanism, in analogy to the thrombin−hirudin interaction (*18*). The lack of significant effects by the alanine mutagenesis of the neutral Q239 thrombin residue is in agreement with this hypothesis. This scenario resembles that one shown in previous studies for the thrombin interaction with other HBS-targeted ligands, namely, prothrombin F_{1+2} and the natural inhibitor haemadin (*19*−*20*). It is of note that all the side chains of the HBS-mutated residues are in "*cis*" configuration, while that of Q239 points to the opposite direction (Figure 6). Besides the electrostatic factor, this aspect might contribute to explain the lack of inhibitory effects by the substitution of this residue. The results confirm that thrombin can interact with different ligands targeted to the same binding site. For F_{1+2}, heparin, hemadin, and GpIb, the ionic interactions play in all cases a relevant role and involve basic residues of the HBS. These are likely engaged in the electrostatic steering of the interacting macromolecules, although a different pattern of electrostatic bonds as well as hydrophobic/stacking components may ensure the specificity of the interaction for the different ligands.

A clear dissociation was observed in the HBS mutants between the changes of the K_d values pertaining to the GpIb interaction, which were severely reduced, and the k_{cat}/K_m values concerning the steady-state PAR1P hydrolysis in solution, which was practically unchanged or even enhanced, as in the case of the Q239A mutant (Table 3). In contrast, the R67A mutant showed a large and similar decrease of the k_{cat}/K_m value both in solution (29-fold) and in situ (19-fold), as expected for a molecule mutated at the FRS which is known to be involved in PAR-1 interaction (*21*), while maintaining WT affinity for GpIb. Moreover, a recent study using the R67Q mutant has also shown that R67 plays a key role in PAR-1 ligation by thrombin (*22*).

The knowledge of both the K_d values of thrombin−GpIb binding and the k_{cat}/K_m values pertaining to PAR1P hydrolysis in solution by mutated thrombins prompted us to investigate the biological activity of these mutants toward intact platelets. The EC_{50} values of thrombin-induced platelet aggregation showed that all the HBS-mutated thrombins, except Q239A, had a reduced platelet activating capacity. The exact mechanism(s) responsible for the effect of HBS mutations on the platelet activation by thrombin can be only partially explained. A recent study has shown in fact that the inhibition of the thrombin−GpIb interaction leads to a reduction of PAR-1 hydrolysis by the enzyme, via a yet unknown mechanism (*5*). Since PAR-1 hydrolysis is considered a key step for the activation of platelets (*23*), this effect may explain, at least in part, why thrombin molecules mutated at the HBS have a reduced capacity to activate platelets. However, it cannot be excluded that the thrombin−GpIb interaction might directly generate second messengers leading to platelet activation or modulation of the PAR signaling pathway(s). Inhibition of the thrombin−GpIb interaction may cause an impairment of this accessory pathway. In fact, a recent study using GpV null mouse platelets, and human platelets rendered deficient in GpV, has demonstrated that enzymatically inactive thrombin, through binding to GpIb, can initiate platelet activation independent of PAR-1 cleavage (*24*). Clearly, further studies are needed to address this issue. In any event, perturbation of the thrombin−GpIb interaction by site-directed alanine mutagenesis of R233, R93, K236, and R233/K236/Q239 was shown to cause a severe reduction of the k_{cat}/K_m value pertaining to the hydrolysis of PAR-1 on intact platelets, while it was unchanged for PAR1P in solution. It is noteworthy that the reduction of the k_{cat}/K_m values of PAR-1 cleavage in situ shown for the HBS mutants was similar to that observed in all the conditions in which the thrombin−GpIb interaction was biochemically impaired, as previously demonstrated (*5*). This result is in agreement with the concept that an optimal cleavage of PAR-1 by thrombin *on the platelet membrane* is positively linked to the thrombin interaction with GpIb (*5*).

In conclusion, a collection of purified alanine thrombin mutants was used to establish that thrombin binds to GpIb through its HBS but does not interact with the FRS. Functional studies showed that some residues, namely, R233, R93, R101, and K236, play a key role in the molecular recognition by GpIb. The alanine substitution of the cationic residues at HBS caused an impairment of the platelet activating capacity arising, at least in part, by a reduced specificity of the PAR-1 hydrolysis in situ. The elucidation of the structural and functional aspects concerning the interaction of thrombin with GpIb may indicate new targets for the development of antithrombotic agents.

ACKNOWLEDGMENT

Stimulating discussions with Prof. T. Pietropaolo (University "Federico II" of Naples, Italy) and with Dr. V. De Filippis (University of Padova, Italy) are gratefully acknowledged.

REFERENCES

1. Clemetson, K., and Clemetson, J. (1995) *Semin. Thromb. Haemost. 21*, 130−137.
2. Buchanan, S. G., and Gay, N. J. (1996) *Prog. Biophys. Mol. Biol. 65*, 1−44.
3. Savage, B., Saldivar, E., and Ruggeri, Z. M. (1996) *Cell 84*, 289−297.
4. Gralnick, H. R., Williams, L. P., McKeown, K., Hansmann, J. W., Fenton, J. W., and Krutzsch, H. (1994) *Proc. Natl. Acad. Sci. U.S.A. 91*, 6334−6338.
5. De Candia, E., Hall, S. H., Rutella, S., Landolfi, R., and De Cristofaro, R. (2001) *J. Biol. Chem. 276*, 4692−4698.
6. Lopez, J. A. (1997) *Blood Coagulation Fibrinolysis 5*, 97−119.
7. Hess, D., Schaller, J., Rickli, E. E., and Clemetson, K. J. (1991) *Eur. J. Biochem. 199*, 389−393.
8. Beer, J. H., Buchi, L., and Steiner, B. (1994) *Blood 83*, 691−702.
9. De Cristofaro, R., De Candia, E., Rutella, S., and Weitz, J. I. (2000) *J. Biol. Chem. 275*, 3887−3895.
10. De Cristofaro, R., De Candia, E., Croce, G., Morosetti, R., and Landolfi, R. (1998) *Biochem. J. 332*, 643−650.
11. Li, C. Q., Vindigni, A., Sadler, J. E., and Wardell, M. R. (2001) *J. Biol. Chem. 276*, 6161−6168.
12. Henriksen, R. A., and Mann, K. G. (1989) *Biochemistry 28*, 2078−2084.
13. Hall, S. W., Nagashima, M., Zhao, L., Morser, J., and Leung, L. L. K. (1999) *J. Biol. Chem. 274*, 25510−6.
14. De Cristofaro, R., and Landolfi, R. (1994) *J. Mol. Biol. 239*, 569−577.
15. De Candia, E., De Cristofaro, R., De Marco, L., Mazzucato, M., Picozzi, M., and Landolfi, R. (1997) *Thromb. Haemostasis 77*, 735−740.
16. Brass, L. F., Pizarro, S., Ahuja, M., Belmonte, E., Blanchard, N., Stadel, J. M., and Hoxie, J. A. (1994) *J. Biol. Chem. 26*, 2943−2952.
17. Bode, W., Turk, D., and Karshikov, A. (1992) *Protein Sci. 1*, 426−471.
18. Stone, S. R., Dennis, S., and Hofsteenge, J. (1989) *Biochemistry 28*, 6857−6863.
19. Arni, R. K., Padmanabhan, K., Padmanabhan, K. P., Wu, T. P., and Tulinsky, A. (1993) *Biochemistry 32*, 4727−4737.
20. Richardson, J. L., Kröger, B., Hoeffken, W., Sadler, J. E., Pereira, P., Huber, R., Bode, W., and Fuentes-Prior, P. (2000) *EMBO J. 19*, 5650−5660.
21. Mathews, I. I., Padmanabhan, K. P., Ganesh, V., Tulinsky, A., Ishii, M., Chen, J., Turck, C. W., Coughlin, S. R., Fenton, J. W., II. (1994) *Biochemistry 33*, 3266−3279.
22. Myles, T., Le Bonniec, B. F., and Stone, S. R. (2001) *Eur. J. Biochem. 268*, 70−77.
23. Coughlin, S. R. (1999) *Proc. Natl. Acad. Sci. U.S.A. 96*, 11023−11027.
24. Ramakrishnan, V., DeGuzman, F., Bao, M., Hall, S. W., Leung, L. L. K., and Phillips, D. R. (2001) *Proc. Natl. Acad. Sci. U.S.A. 98*, 1823−1828.

BI010491F